Noncollinear Magnetic Order Stabilized by Entangled Spin-Orbital Fluctuations

Wojciech Brzezicki,[1] Jacek Dziarmaga,[1] and Andrzej M. Oleś[1,2]

[1]*Marian Smoluchowski Institute of Physics, Jagellonian University, Reymonta 4, PL-30059 Kraków, Poland*
[2]*Max-Planck-Institut für Festkörperforschung, Heisenbergstrasse 1, D-70569 Stuttgart, Germany*

(Received 15 August 2012; published 3 December 2012)

Quantum phase transitions in the two-dimensional Kugel-Khomskii model on a square lattice are studied using the plaquette mean field theory and the entanglement renormalization *Ansatz*. When $3z^2$-r^2 orbitals are favored by the crystal field and Hund's exchange is finite, both methods give a noncollinear exotic magnetic order that consists of four sublattices with mutually orthogonal nearest-neighbor and antiferromagnetic second-neighbor spins. We derive an effective frustrated spin model with second- and third-neighbor spin interactions which stabilize this phase and follow from spin-orbital quantum fluctuations involving spin singlets entangled with orbital excitations.

DOI: 10.1103/PhysRevLett.109.237201 PACS numbers: 75.10.Jm, 03.65.Ud, 64.70.Tg, 75.25.Dk

Introduction.—Almost 40 years ago Kugel and Khomskii realized that spins and orbitals should be treated on equal footing in Mott insulators with active orbital degrees of freedom [1]. Their model qualitatively explains the magnetic and orbital order in $KCuF_3$, which is a well-known example for spinon excitations in a one-dimensional (1D) antiferromagnetic (AF) Heisenberg chain [2]. This archetypal compound is usually given as an example of the spin-orbital physics [3], which covers a broad class of transition metal compounds, including perovskite manganites [4], titanates [5], vanadates [6], ruthenates [7], 1D cuprates [8], layered ruthenates [9], and pnictide superconductors [10]. In all these compounds, strong intraorbital Coulomb repulsion U dominates over electron hopping t ($t \ll U$), and charge fluctuations are suppressed. On the one hand, spin degrees of freedom may separate from the orbitals when the coupling to the lattice is strong, as in $LaMnO_3$ [4] and recently shown to also happen in $KCuF_3$ [11]. On the other hand, the spin-orbital quantum fluctuations are strongly enhanced for low $S = \frac{1}{2}$ spins, as in the three-dimensional (3D) Kugel-Khomskii (KK) model [12,13], and lead to a spin-orbital liquid phase in $LaTiO_3$ [5]. Geometrical frustration [14] was also suggested as a stabilizing mechanism for a spin-orbital liquid phase [15], with examples on a triangular lattice in e_g ($LiNiO_2$ [16]) and t_{2g} ($LiNiO_2$ [17]) orbital systems. Frustrated spin-orbital interactions to further neighbors may also destabilize long-range magnetic order [18]. An opposite case when orbital excitations determine the spin order has not been reported until now.

The phase diagram of the 3D KK model remains controversial in the regime of strongly frustrated interactions-it has been suggested that either spin-orbital fluctuations destabilize long-range spin order [12] or an orbital gap opens and stabilizes spin order [13]. This difficulty is typical for systems with spin-orbital entanglement [19], which may occur both in the ground state [20] and in excited states [21]. The best known examples are the 1D [22] or two-dimensional (2D) [23] SU(4) models, where spin and orbital operators appear in a symmetric way. Instead, the symmetry in the orbital sector is much lower, and orbital excitations measured in $KCuF_3$ [24] are expected to be inherently coupled to spin fluctuations [25].

In this Letter, we present a surprising noncollinear spin order in the 2D KK model that goes beyond mean field studies [26] and explain its origin. So far, noncollinear spin order has been obtained for frustrated exchange in Kondo-lattice models on square lattices, without [27] and with [28] orbital degeneracy, or at finite spin-orbit coupling [29]. In MnV_2O_4 spinel, it is accompanied by a structural distortion and the orbital order [30]. Here, we find yet a different situation: when frustrated nearest-neighbor (NN) exchange terms almost compensate each other and orbitals are in the ferro-orbital (FO) state, the spin order follows from further neighbor spin interactions triggered by entangled spin-orbital excitations.

Variational approach.—We begin by presenting two general variational methods for spin-orbital systems: (i) the plaquette mean field (PMF) *Ansatz* [see Fig. 1(a)] and (ii) the entanglement renormalization *Ansatz* (ERA)

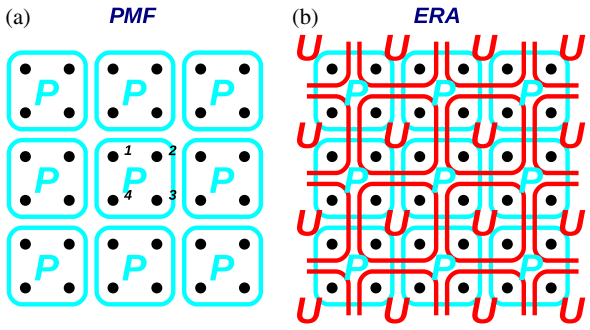

FIG. 1 (color online). Two variational *Ansätze* used in the present Letter: (a) PMF and (b) ERA. Black dots are lattice sites, $\mathcal{P}$'s are variational wave functions on 2×2 plaquettes, and $\mathcal{U}$'s are variational 2×2 unitary disentanglers.

[31] [see Fig. 1(b)]. In the PMF, adapted here from a similar method for the bilayer KK model [32], one employs a variational *Ansatz* in the form of a product of plaquette 2×2 wave functions $\mathcal{P}$'s [33]. Energy is minimized with respect to $\mathcal{P}$'s to obtain the best approximation to the ground state. The ERA is a refined version of the PMF, where the product of the $\mathcal{P}$'s is subject to an additional unitary transformation, being a product of 2×2 "disentanglers" $\mathcal{U}$. They introduce entanglement between different plaquettes and make the ERA more accurate.

Kugel-Khomskii model and methods.—The perturbation theory for a Mott insulator with active e_g orbitals in the regime of $t \ll U$ leads to the spin-orbital model [34], with the Heisenberg SU(2) spin interactions coupled to the orbital operators for the holes in the d^9 ionic states,

$$\mathcal{H} = -\frac{1}{2}J\sum_{\langle ij\rangle\|\gamma}\left\{(r_1\Pi_t^{(ij)} + r_2\Pi_s^{(ij)})\left(\frac{1}{4} - \tau_i^\gamma\tau_j^\gamma\right) + (r_3 + r_4)\Pi_s^{(ij)}\left(\frac{1}{2} - \tau_i^\gamma\right)\left(\frac{1}{2} - \tau_j^\gamma\right)\right\} + \mathcal{H}_0. \quad (1)$$

Each bond $\langle ij\rangle$ connects NN sites $\{i, j\}$ along one of the orthogonal axes $\gamma = a, b$ in the ab plane. The model describes the spin-orbital superexchange in K_2CuF_4 [35], with the superexchange constant $J = 4t^2/U$. The coefficients $r_1 \equiv 1/(1-3\eta)$, $r_2 = r_3 \equiv 1/(1-\eta)$, and $r_4 \equiv 1/(1+\eta)$ refer to the $d_i^9 d_j^9 \rightleftharpoons d_i^8 d_j^{10}$ charge excitations to the upper Hubbard band [34] and depend on Hund's exchange parameter

$$\eta = \frac{J_H}{U}. \quad (2)$$

The spin projection operators Π_{ij}^s and Π_{ij}^t select a singlet (Π_{ij}^s) or triplet (Π_{ij}^t) configuration for spins $S = 1/2$ on the bond $\langle ij\rangle$, respectively,

$$\Pi_s^{(ij)} = \left(\frac{1}{4} - \mathbf{S}_i\cdot\mathbf{S}_j\right), \qquad \Pi_t^{(ij)} = \left(\frac{3}{4} + \mathbf{S}_i\cdot\mathbf{S}_j\right). \quad (3)$$

Here, τ_i^γ act in the subspace of e_g orbitals occupied by a hole $\{|x\rangle, |z\rangle\}$, with $|z\rangle \equiv (3z^2 - r^2)/\sqrt{6}$ and $|x\rangle \equiv (x^2 - y^2)/\sqrt{2}$, and they can be expressed in terms of Pauli matrices $\{\sigma_i^x, \sigma_i^z\}$ in the following way [34]:

$$\tau_i^{a(b)} \equiv \frac{1}{4}\left(-\sigma_i^z \pm \sqrt{3}\sigma_i^x\right), \qquad \tau_i^c = \frac{1}{2}\sigma_i^z. \quad (4)$$

The term $\mathcal{H}_0$ in Eq. (1) is the crystal field splitting of two e_g orbitals induced by the lattice geometry or pressure,

$$\mathcal{H}_0 = -E_z\sum_i \tau_i^c. \quad (5)$$

When $|E_z| \gg J$, it dictates the FO order with either z or x orbitals as long as we stay in the AF regime, see Fig. 2. This ground state can be further improved using perturbation theory in a dimensionless parameter $|\varepsilon_z|^{-1} \equiv J/|E_z|$.

In the PMF, one finds self-consistently mean fields: $s_i^\alpha \equiv \langle S_i^\alpha\rangle$, $t_i^\gamma \equiv \langle\tau_i^\gamma\rangle$, and $v_i^{\alpha,\gamma} \equiv \langle S_i^\alpha\tau_i^\gamma\rangle$. Here, $\gamma = a, b$, $\alpha = x, z$, and $i = 1, \ldots, 4$ labels sites of a single plaquette; see Fig. 1(a). We assume that either all plaquettes are the same or that the neighboring plaquettes are rotated by $\pi/2$ with respect to each other in the ab plane. In the latter case, the order parameters are interchanged ($a \leftrightarrow b$) between neighboring plaquettes and transform as $\{t_i^{a(b)}\} \rightarrow \{t_i^{b(a)}\}$ and $\{v_i^{\alpha,a(b)}\} \rightarrow \{v_i^{\alpha,b(a)}\}$. In the ERA treatment we either assume that all $\mathcal{P}$'s and $\mathcal{U}$'s are the same, as in Fig. 1(b), or divide the plaquette lattices of $\mathcal{P}$'s and $\mathcal{U}$'s into four sublattices with four independent $\mathcal{P}$'s and $\mathcal{U}$'s. One finds that the energy found in the ERA, when optimized with respect to both $\mathcal{U}$ and $\mathcal{P}$, is typically 5–15% lower than that found in the PMF.

Phase diagram.—The phase diagram in the (ε_z, η) plane contains six phases; see Fig. 2. The same phases appear in both the PMF and ERA, which suggests that the phase diagram is complete. At large η values one finds two FM phases: either with alternating orbital (AO) order as observed in K_2CuF_4 [36,37] or with FOz order (FMz). At $E_z < -1.8J$, a second-order transition occurs from the FM to the FMz phase (all other transitions involve both spins, and orbitals are first order) at $\varepsilon_z/r_1 = -0.934$ (-0.837) in the PMF (ERA). In these phases, $\Pi_t^{(ij)} = 1$ and the Hamiltonian (1) reduces to the e_g orbital model [38] or to the generalized compass model [39], in transverse field E_z. At $E_z = 0$, one finds AO order with $\langle\sigma^x\rangle \neq 0$, while finite E_z induces transverse polarization $\langle\sigma^z\rangle \neq 0$.

The phase diagram includes also two AF phases. They have uniform FO order with $\langle\sigma^z\rangle > 0$ for $E_z > 0$ and

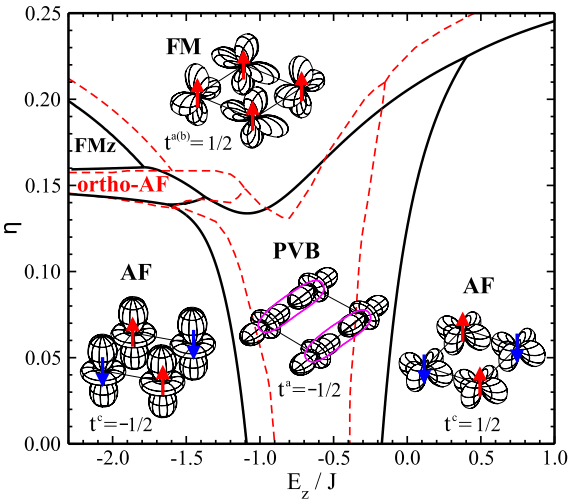

FIG. 2 (color online). Phase diagram of the 2D KK model in the PMF (solid lines) and ERA (dashed lines) variational approximations. Insets show representative spin and orbital configurations on a 2×2 plaquette: x-like ($t^c = \frac{1}{2}$) and z-like ($t^{a,c} = -\frac{1}{2}$) orbitals [47] are accompanied either by AF spin order (arrows) or by spin singlets in the PVB phase (ovals). The FM phase has a two-sublattice AO order (with $t^{a(b)} = \frac{1}{2}$ at $E_z = 0$) or FOz order (FMz). Between the AF and FM (FMz) phase one finds an exotic ortho-AF phase-it has a noncollinear spin order; see text.

$\langle\sigma^z\rangle < 0$ for $E_z < 0$. The spin interactions in two AF phases are nonequivalent and are much weaker for $E_z < 0$ than for $E_z > 0$; this difference increases up to a factor of 9 for fully polarized orbitals [40]. These two phases are separated by the plaquette valence bond (PVB) phase with pairs of parallel spin singlets, horizontal or vertical and alternating between NN plaquettes. Note that the PVB phase is an analogue of spin liquid phases found before for the 3D KK model [12] and the bilayer [32].

Finally, at $E_z < 0$ and $\eta \sim 0.15$, we find a novel exotic "orthogonal AF" ("ortho-AF") phase with entanglement ($v_i^{\alpha,\gamma} \neq s_i^\alpha t_i^\gamma$) that emerges between the AF and FM (FMz) phases. This state is characterized by the noncollinear magnetic order (see Fig. 3), with NN spins being orthogonal to each other and next-nearest neighbor (NNN) spins being AF. This phase is robust and has a somewhat extended range of stability in the ERA. In contrast to the frustrated spin J_1-J_2 interactions on a square lattice [41], one finds here that J_1 is negligible and spin order follows from further neighbor couplings.

Effective spin model.—To explain the exotic magnetic order in the ortho-AF phase shown in Fig. 3, we derive an effective spin model for this phase. We show that NNN and third NN (3NN) spin interactions emerge here from the frustrated spin-orbital superexchange, $\mathcal{V} \equiv \mathcal{H} - \mathcal{H}_0$, treated as perturbation of the orbital ground state $|0\rangle$ of the unperturbed Hamiltonian $\mathcal{H}_0$ (5). Note an analogy to hidden multiple-spin interactions derived recently for frustrated Kondo-lattice models [42].

For negative $\varepsilon_z < 0$, the ground state $|0\rangle$ of $\mathcal{H}_0$ is the FOz state with z orbitals occupied by a hole at each site, $\tau_i^c|0\rangle = -\frac{1}{2}|0\rangle$, and the energy $\varepsilon_0 = -\frac{1}{2}|\varepsilon_z|$ per site. A finite gap that occurs for orbital excitations helps to remove high spin degeneracy in $|0\rangle$ by effective spin interactions in the Hamiltonian H_s that can be constructed using the expansion in powers of $|\varepsilon_z|^{-1}$,

$$H_s \simeq J\{N\varepsilon_0 + H_s^{(1)} + H_s^{(2)} + H_s^{(3)}\}, \tag{6}$$

where N is the number of sites. The first-order term is an average $H_s^{(1)} \equiv \langle 0|\mathcal{V}|0\rangle$. Similarly, to evaluate $H_s^{(2)}$ and $H_s^{(3)}$, we determine the matrix elements $\langle n|\mathcal{V}|0\rangle$ for the excited states $|n\rangle$ with a certain number of z orbitals flipped to x orbitals. All the averages are taken between orbital states, and the spin model Eq. (6) follows.

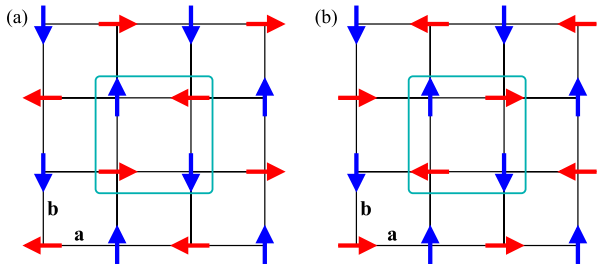

FIG. 3 (color online). Schematic view of two nonequivalent spin configurations (a) and (b) of the classical ortho-AF phase $|\mathrm{AF}_\perp\rangle$, which cannot be transformed one into the other by lattice translations. Four spin directions (arrows) correspond to four spin sublattices: up or down arrows stand for eigenstates of $\langle S_i^z\rangle = \pm\frac{1}{2}$, whereas right or left arrows stand for $\langle S_i^x\rangle = \pm\frac{1}{2}$.

The first order yields the Heisenberg Hamiltonian

$$H_s^{(1)} = \frac{1}{2^5}(-3r_1 + 4r_2 + r_4)\sum_{\langle ij\rangle}(\mathbf{S}_i \cdot \mathbf{S}_j). \tag{7}$$

The NN interaction $J_1 \equiv (-3r_1 + 4r_2 + r_4)J/2^5$ changes sign at $\eta_0 \simeq 0.155$, implying a direct AF-FM transition. However, this turns out to be a premature conclusion because the vanishing of $H_s^{(1)}$ at η_0 makes higher-order terms in Eq. (6) relevant. Indeed, η_0 nicely falls into the ortho-AF area of the phase diagram in Fig. 2, where the NN interaction J_1 is small and frustrated.

Higher-order terms.—Higher-order terms arise by flipping orbitals from the ground state $|0\rangle$. Given that $\mathcal{V}$ has nonzero overlap only with states having one or two NN orbitals flipped from z to x, one finds in second order

$$H_s^{(2)} = \frac{\xi(\eta)}{|\varepsilon_z|}\Big\{\sum_{\langle\langle ij\rangle\rangle}(\mathbf{S}_i \cdot \mathbf{S}_j) - \frac{1}{2}\sum_{\langle\langle\langle ij\rangle\rangle\rangle}(\mathbf{S}_i \cdot \mathbf{S}_j)\Big\}, \tag{8}$$

with $\xi(\eta) = (r_1 + 2r_2 + 3r_4)^2/2^{10}$. Here, $\langle\langle ij\rangle\rangle$ and $\langle\langle\langle ij\rangle\rangle\rangle$ stand for NNN and 3NN sites i and j; see Fig. 4(a) for the origin and sign of these interactions. Apart from this, the second order also brings the $|\varepsilon_z|^{-1}$ correction to the Heisenberg interactions of $H_s^{(1)}$ (7), moving the transition point from η_0 to $\eta_0 + O(\varepsilon_z^{-1})$.

The NNN AF interaction in $H_s^{(2)}$ (8) alone would give two quantum antiferromagnets on interpenetrating sublattices [43], but the additional 3NN FM term makes these AF states more classical than in the 2D Heisenberg model (Supplemental Material [44]). This "double-AF" configuration is already similar to the ortho-AF phase in Fig. 3. However, the second order does not explain why the spins in the ortho-AF phase prefer to be orthogonal on NN bonds, and we have to proceed to the third order.

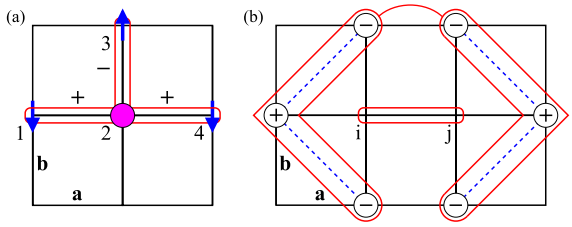

FIG. 4 (color online). Artist's views of the effective spin interactions obtained in (a) second-order $H_s^{(2)}$, with NNN term (123) and 3NN term (124), and (b) third-order $H_s^{(3)}$. The frames in (a) indicate Heisenberg bonds multiplied along a or b axes with $\pm$ sign depending on the bond direction; the dot in the center stands for an orbital flip in $|0\rangle$. In (b) the dashed lines symbolize sums of three spins which enter each effective spin, $\mathbf{S}_{\mathcal{N}_\gamma(i)}$ and $\mathbf{S}_{\mathcal{N}_{\bar\gamma}(j)}$; the phase factors s_γ (circles) and their scalar product are marked with connected frames.

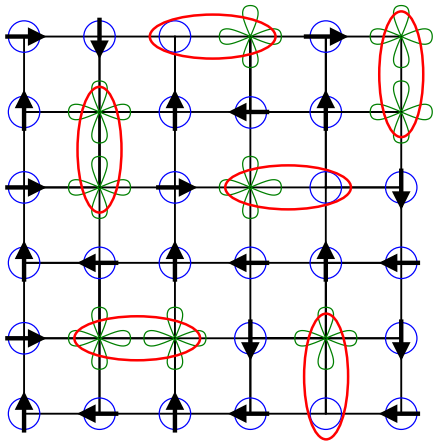

FIG. 5 (color online). Artist's view of the ortho-AF state $|\Psi_{\rm SO}\rangle$ (10), with spin order (arrows) of Fig. 3 and FOz orbital order (circles) in the ab plane. The state is dressed with spin singlets (ovals) entangled with either one or two orbital excitations from $|z\rangle$ to $|x\rangle$ orbitals (clovers) on NN bonds.

The third order in Eq. (6) produces many contributions to the spin Hamiltonian, but we are interested only in qualitatively new terms comparing to the lower orders. The terms bringing potentially new physics are the ones with connected products of three different Heisenberg bonds (Supplemental Material [44]). The final result is a four-spin coupling,

$$H_{\perp}^{(3)} = \frac{1}{\varepsilon_z^2}\chi(\eta)\xi(\eta)\sum_{\langle ij\rangle||\gamma}(\mathbf{S}_i\cdot\mathbf{S}_j)(\mathbf{S}_{\mathcal{N}_\gamma(i)}\cdot\mathbf{S}_{\mathcal{N}_{\bar\gamma}(j)}), \quad (9)$$

where $\bar\gamma = -\gamma$ and $\mathbf{S}_{\mathcal{N}_\gamma(i)} \equiv \sum_{\alpha\neq\gamma} s_\alpha \mathbf{S}_{i+\alpha}$ is an effective spin around site i in the direction γ; see Fig. 4(b). Here, $\chi(\eta) = 9(r_1 + r_4)/2^7$, $\alpha \in \{\pm a, \pm b\}$, and $s_\alpha = -1$ for $\alpha = \pm b$ and $s_\alpha = 1$ otherwise. In the limit of two interpenetrating classical antiferromagnets, $H_\perp^{(3)}$ gives the energy per site, $\varepsilon_\perp^{(3)} \approx \varepsilon_z^{-2}\chi(\eta)\xi(\eta)(\frac{3}{4}\cos\varphi)^2$, where φ is an angle between the NN spins (Supplemental Material [44]). This classical energy is minimized for $\varphi = \pi/2$, which explains the exotic magnetic order in the ortho-AF phase, shown in Fig. 3.

Spin-orbital entanglement.—The ground state $|\mathrm{AF}_\perp\rangle$ of H_s (6) is nearly classical, except for small quantum corrections obtained within the spin-wave expansion (see the Supplemental Material [44]). Thus, one might expect that the spins are not entangled with orbitals. However, this argument overlooks that the resulting spins in H_s are dressed with orbital and spin-orbital fluctuations. Indeed, within the perturbative treatment we obtain the full spin-orbital ground state,

$$|\Psi_{\rm SO}\rangle \propto \Big(1 - \sum_{n\neq 0}\frac{\mathcal{V}_n}{\varepsilon_n} + \sum_{n,m\neq 0}\frac{\mathcal{V}_n\mathcal{V}_m}{\varepsilon_n\varepsilon_m} - \cdots\Big)|\Phi_0\rangle, \quad (10)$$

where $\mathcal{V}_n \equiv |n\rangle\langle n|\mathcal{V}$, ε_n are excitation energies and $|\Phi_0\rangle \equiv |\mathrm{AF}_\perp\rangle|0\rangle$ is the disentangled classical state (Fig. 3). The operator sum in front of $|\Phi_0\rangle$ dresses this state with both orbital and spin-orbital fluctuations. When the purely orbital fluctuations are neglected and density of spin-orbital defects is assumed to be small, one finds

$$|\Psi_{\rm SO}\rangle \simeq \exp\Big(-\frac{1}{|\varepsilon_z|}\sum_{\langle ij\rangle||\gamma}\mathcal{D}_{ij}^{\gamma}\Big)|\Phi_0\rangle, \quad (11)$$

where

$$\mathcal{D}_{ij}^{\gamma} = \{-A\sigma_i^x\sigma_j^x + B(\sigma_i^x + \sigma_j^x)s_\gamma\}\Pi_{ij}^s \quad (12)$$

is the spin-orbital excitation operator on the bond $\langle ij\rangle$, with $A = 3(r_1 + r_4)/2^6$ and $B = \sqrt{3}(r_1 + 2r_2 + 3r_4)/2^5$. Both terms in Eq. (12) project on a NN spin singlet, but the first one flips two NN z orbitals while the second one generates only one flipped orbital. In short, the exponent $e^{-D/|\varepsilon_z|}$ dresses the classical ortho-AF state $|\mathrm{AF}_\perp\rangle$ in Fig. 3 with the entangled (spin-singlet and one or two flipped orbitals) defects; see Fig. 5. The density of such entangled defects increases when $|\varepsilon_z|$ is decreased towards the PVB phase.

Topological defects.—The order parameter of the ortho-AF phase has nontrivial topology. The ground state is degenerate with respect to different orientations of its order parameter that consist of two orthogonal unit vectors defining the orientation of each antiferromagnet. The first vector lives on the whole sphere S^2, but the second one is restricted to a circle S^1 because it is orthogonal to the first. In addition to spin-wave excitations, this $S^2 \times S^1$ topology allows for Skyrmions (textures) [45] and $\mathbb{Z}_2$ vortices (hedgehogs) as two types of topological defects. The hedgehog is stabilized by the orthogonality of the antiferromagnets. For instance, when one of them has fixed uniform orientation of its Néel order in space, the orthogonal orientation of the other one is free to make a hedgehoglike rotation.

Summary.—We have found surprising *noncollinear* spin order that arises from the NN spin-orbital superexchange when ferromagnetic and antiferromagnetic interactions almost compensate each other in the 2D KK model away from orbital degeneracy. It is stabilized by further neighbor spin exchange generated by entangled spin-orbital fluctuations, which involve spin singlets and orbital flips. A similar mechanism works in the 3D KK model, where it leads to a rich variety of spin-orbital phases, to be reported elsewhere.

Finally, we note that magnetic order in spin-orbital systems may be changed by applying pressure [46]—indeed, a transition from ferromagnetic to antiferromagnetic order was observed in K_2CuF_4 [36,37]. Such a transition is also found here for a realistic value of $\eta \simeq 0.15$, and one could induce it in the antiferromagnetic phase by external magnetic field. Whether the antiferromagnetic order could be noncollinear as predicted here remains an experimental challenge.

We thank G. Khaliullin, R. Kremer, and B. Normand for insightful discussions. This work was supported by the Polish National Science Center (NCN) under Projects No. 2012/04/A/ST3/00331 (W. B. and A. M. O.) and No. 2011/01/B/ST3/00512 (J. D.).

[1] K. I. Kugel and D. I. Khomskii, Sov. Phys. JETP **37**, 725 (1973); Sov. Phys. Usp. **25**, 231 (1982).

[2] B. Lake, D. A. Tennant, and S. E. Nagler, Phys. Rev. B **71**, 134412 (2005); B. Lake, D. A. Tennant, C. D. Frost, and S. E. Nagler, Nat. Mater. **4**, 329 (2005).

[3] Y. Tokura and N. Nagaosa, Science **288**, 462 (2000).

[4] L. F. Feiner and A. M. Oleś, Phys. Rev. B **59**, 3295 (1999).

[5] G. Khaliullin and S. Maekawa, Phys. Rev. Lett. **85**, 3950 (2000); G. Jackeli and G. Khaliullin, *ibid.* **101**, 216804 (2008).

[6] G. Khaliullin, P. Horsch, and A. M. Oleś, Phys. Rev. Lett. **86**, 3879 (2001); Phys. Rev. B **70**, 195103 (2004).

[7] Z. Fang, K. Terakura, and N. Nagaosa, New J. Phys. **7**, 66 (2005).

[8] J. Schlappa *et al.*, Nature (London) **485**, 82 (2012).

[9] M. Cuoco, F. Forte, and C. Noce, Phys. Rev. B **74**, 195124 (2006); F. Forte, M. Cuoco, and C. Noce, *ibid.* **82**, 155104 (2010).

[10] F. Krüger, S. Kumar, J. Zaanen, and J. van den Brink, Phys. Rev. B **79**, 054504 (2009).

[11] J. C. T. Lee *et al.*, Nat. Phys. **8**, 63 (2012).

[12] L. F. Feiner, A. M. Oleś, and J. Zaanen, Phys. Rev. Lett. **78**, 2799 (1997); J. Phys. Condens. Matter **10**, L555 (1998).

[13] G. Khaliullin and V. Oudovenko, Phys. Rev. B **56**, R14243 (1997).

[14] L. Balents, Nature (London) **464**, 199 (2010).

[15] V. Fritsch, J. Hemberger, N. Büttgen, E.-W. Scheidt, H.-A. Krug von Nidda, A. Loidl, and V. Tsurkan, Phys. Rev. Lett. **92**, 116401 (2004); A. Krimmel, M. Mücksch, V. Tsurkan, M. M. Koza, H. Mutka, and A. Loidl, *ibid.* **94**, 237402 (2005).

[16] F. Vernay, K. Penc, P. Fazekas, and F. Mila, Phys. Rev. B **70**, 014428 (2004); F. Vernay, A. Ralko, F. Becca, and F. Mila, *ibid.* **74**, 054402 (2006).

[17] B. Normand and A. M. Oleś, Phys. Rev. B **78**, 094427 (2008); B. Normand, *ibid.* **83**, 064413 (2011); J. Chaloupka and A. M. Oleś, *ibid.* **83**, 094406 (2011).

[18] S. Nakatsuji *et al.*, Science **336**, 559 (2012).

[19] A. M. Oleś, J. Phys. Condens. Matter **24**, 313201 (2012).

[20] A. M. Oleś, P. Horsch, L. F. Feiner, and G. Khaliullin, Phys. Rev. Lett. **96**, 147205 (2006); Y. Chen, Z. D. Wang, Y. Q. Li, and F. C. Zhang, Phys. Rev. B **75**, 195113 (2007).

[21] J. Sirker, A. Herzog, A. M. Oleś, and P. Horsch, Phys. Rev. Lett. **101**, 157204 (2008); G.-W. Chern and N. Perkins, Phys. Rev. B **80**, 180409 (2009); W.-L. You, A. M. Oleś, and P. Horsch, *ibid.* **86**, 094412 (2012).

[22] Y. Q. Li, M. Ma, D. N. Shi, and F. C. Zhang, Phys. Rev. Lett. **81**, 3527 (1998).

[23] F. Wang and A. Vishwanath, Phys. Rev. B **80**, 064413 (2009).

[24] K. Ishii *et al.*, Phys. Rev. B **83**, 241101 (2011).

[25] K. Wohlfeld, M. Daghofer, S. Nishimoto, G. Khaliullin, and J. van den Brink, Phys. Rev. Lett. **107**, 147201 (2011).

[26] J. Chaloupka and G. Khaliullin, Phys. Rev. Lett. **100**, 016404 (2008).

[27] M. Yamanaka, W. Koshibae, and S. Maekawa, Phys. Rev. Lett. **81**, 5604 (1998); H. Aliaga, B. Normand, K. Hallberg, M. Avignon, and B. Alascio, Phys. Rev. B **64**, 024422 (2001); J. W. F. Venderbos, M. Daghofer, J. van den Brink, and S. Kumar, Phys. Rev. Lett. **109**, 166405 (2012).

[28] J. Lorenzana, G. Seibold, C. Ortix, and M. Grilli, Phys. Rev. Lett. **101**, 186402 (2008).

[29] J. Yamaura *et al.*, Phys. Rev. Lett. **108**, 247205 (2012).

[30] V. O. Garlea, R. Jin, D. Mandrus, B. Roessli, Q. Huang, M. Miller, A. J. Schultz, and S. E. Nagler, Phys. Rev. Lett. **100**, 066404 (2008).

[31] G. Vidal, Phys. Rev. Lett. **99**, 220405 (2007); **101**, 110501 (2008); L. Cincio, J. Dziarmaga, and M. M. Rams, *ibid.* **100**, 240603 (2008); see also Fig. 23 in G. Evenbly and G. Vidal, Phys. Rev. B **79**, 144108 (2009).

[32] W. Brzezicki and A. M. Oleś, Phys. Rev. B **83**, 214408 (2011); W. Brzezicki and A. M. Oleś, Acta Phys. Pol. A **121**, 1045 (2012).

[33] This choice is motivated by a particular preference towards spin singlets with $|z\rangle$-like orbitals on the bonds.

[34] A. M. Oleś, L. F. Feiner, and J. Zaanen, Phys. Rev. B **61**, 6257 (2000).

[35] M. V. Mostovoy and D. I. Khomskii, Phys. Rev. Lett. **92**, 167201 (2004).

[36] M. Ishizuka, I. Yamada, K. Amaya, and S. Endo, J. Phys. Soc. Jpn. **65**, 1927 (1996).

[37] M. Ishizuka, M. Terai, S. Endo, M. Hidaka, I. Yamada, and O. Shimomura, J. Magn. Magn. Mater. **177–181**, 725 (1998); M. Ishizuka, M. Terai, M. Hidaka, S. Endo, I. Yamada, and O. Shimomura, Phys. Rev. B **57**, 64 (1998).

[38] J. van den Brink, P. Horsch, F. Mack, and A. M. Oleś, Phys. Rev. B **59**, 6795 (1999); W.-L. You, G.-S. Tian, and H.-Q. Lin, *ibid.* **75**, 195118 (2007).

[39] L. Cincio, J. Dziarmaga, and A. M. Oleś, Phys. Rev. B **82**, 104416 (2010).

[40] Due to this difference the ortho-AF phase exists in a more restricted range for $E_z > 0$: $\eta \simeq 0.29$ and $E_z > 3J$.

[41] R. R. P. Singh, Z. Weihong, C. J. Hamer, and J. Oitmaa, Phys. Rev. B **60**, 7278 (1999); B. Schmidt, M. Siahatgar, and P. Thalmeier, *ibid.* **83**, 075123 (2011).

[42] Y. Akagi, M. Udagawa, and Y. Motome, Phys. Rev. Lett. **108**, 096401 (2012).

[43] The spin interactions of Eq. (8) exclude the spiral order.

[44] See the Supplemental Material at http://link.aps.org/supplemental/10.1103/PhysRevLett.109.237201 for more technical details.

[45] F. Wilczek and A. Zee, Phys. Rev. Lett. **51**, 2250 (1983); D. A. Abanin, S. A. Parameswaran, and S. L. Sondhi, *ibid.* **103**, 076802 (2009).

[46] Y. Ding, D. Haskel, Y.-C. Tseng, E. Kaneshita, M. van Veenendaal, J. F. Mitchell, S. V. Sinogeikin, V. Prakapenka, and H.-k. Mao, Phys. Rev. Lett. **102**, 237201 (2009); J.-S. Zhou, J. B. Goodenough, J.-Q. Yan, J.-G. Cheng, K. Matsubayashi, Y. Uwatoko, and Y. Ren, Phys. Rev. B **80**, 224422 (2009).

[47] In fact, the orbitals are never fully polarized; e.g., considering finite Hund's exchange $\eta = 0.05$ we get $t^c \simeq -0.496$ for $E_z = -2J$ in the left AF phase, $t^c \simeq 0.487$ for $E_z = 1J$ in the right AF phase, and $t^a \simeq -0.466$ for $E_z = -0.5J$ in the PVB phase, where the deviations from $t^a = -\frac{1}{2}$ are typically larger.